The National Direct-Drive Inertial Confinement Fusion Program

S. P. REGAN [1], V. N. GONCHAROV [1], T. C. SANGSTER [1], E. M. CAMPBELL [1], R. BETTI [1], J. W. BATES [2] K. BAUER [1], T. BERNAT [3], S. BHANDARKAR [4], T. R. BOEHLY [1], M. J. BONINO [1], A. BOSE [1], D. CAO [1], R. CHAPMAN [1], T. CHAPMAN [4], G. W. COLLINS [1], T. J. B. COLLINS [1], R. S. CRAXTON [1], J. A. DELETTREZ [1], D. H. EDGELL [1], R. EPSTEIN [1], M. FARRELL [5], C. J. FORREST [1], R. K. FOLLETT [1], J. A. FRENJE [6], D. H. FROULA [1], M. GATU JOHNSON [6], C. R. GIBSON [5], C. GOYON [4], V. Yu. GLEBOV [1], A. GREENWOOD[5], D. R. HARDING [1], M. HOHENBERGER [4], S. X. HU [1], H. HUANG [5], J. HUND [3], I. V. IGUMENSHCHEV [1], D. W. JACOBS-PERKINS [1], R. T. JANEZIC [1], M. KARASIK [2], J. H. KELLY [1], T. J. KESSLER [1], J. P. KNAUER [1], T. Z. KOSC [1], S. J. LOUCKS [1], J. A. MAROZAS [1], F. J. MARSHALL [1], R. L. MCCRORY [1], P. W. MCKENTY [1], D. T. MICHEL [1], P. MICHEL [4], J. D. MOODY [4], J. F. MYATT [1], A. NIKROO [4], P. M. NILSON [1], S. P. OBENSCHAIN [2], J. P. PALASTRO [1], J. PEEBLES [1], R. D. PETRASSO [6], N. PETTA [3], P. B. RADHA [1], J. E. RALPH [4], M. J. ROSENBERG [1], S. SAMPAT [1], A. J. SCHMITT [2], M. J. SCHMITT [7], M. SCHOFF [5], W. SEKA [1], R. SHAH [1], J. R. RYGG [1], J. G. SHAW [1], R. SHORT [1], W. T. SHMAYDA [1], M. J. SHOUP III [1], A. SHVYDKY[1], A. A. SOLODOV [1], C. SORCE [1], M. STADERMANN [4], C. STOECKL [1], W. SWEET [5], C. TAYLOR [1], R. TAYLOR [1], W. THEOBALD [1], D. P. TURNBULL [1], J. ULREICH [1], M. D. WITTMAN [1], K. M. WOO [1], and J. D. ZUEGEL [1]

1) Laboratory for Laser Energetics, University of Rochester, USA

E-mail: sreg@lle.rochester.edu

2) Naval Research Laboratory, USA

3) Schafer Corporation, USA

4) Lawrence Livermore National Laboratory, USA

5) General Atomics, USA

6) Plasma Science and Fusion Center, Massachusetts Institute of Technology, USA

7) Los Alamos National Laboratory, USA

ABSTRACT

The National Direct-Drive Inertial Confinement Fusion Program consists of the 100-Gbar Campaign on the 30-kJ, 351-nm, 60-beam OMEGA Laser System and the MegaJoule Direct Drive (MJDD) Campaign on the 1.8-MJ, 351-nm, 192-beam National Ignition Facility (NIF). The main goals of the 100-Gbar Campaign are to demonstrate and understand the physics for hot-spot conditions and formation relevant for ignition at the MJ scale, while the MJDD Campaign seeks to understand the laser plasma interactions, energy coupling, and laser imprint for ignition-scale direct-drive coronal plasmas. An overview of the multi-year, systematic effort that is underway for the National Direct-Drive Inertial Confinement Fusion Program, including laser, target, and diagnostic improvements that are in progress, as well as recent results from the 100-Gbar Campaign on OMEGA and MJDD Campaign on NIF are presented.

I. INTRODUCTION

The National Direct-Drive Program [1-3] is underway on 30-kJ, 351-nm, 60-beam OMEGA laser [4] and at the 1.8-MJ, 351-nm, 192-beam National Ignition Facility (NIF) [5]. Laser Direct Drive (LDD) [1-3, 6] is one of the three inertial confinement fusion (ICF) approaches being explored to achieve ignition [7]. The 100-Gbar Campaign on OMEGA explores the formation of hot-spot conditions relevant for ignition at the MJ scale using hydrodynamically-scaled implosions of layered DT cryogenic targets [1-3]. The enhanced-capability approach of the 100-Gbar Campaign involves improvements to OMEGA laser [1-3], targets [8], diagnostics [9-12], and new modeling and simulation capabilities [13-18] to increase the areal density and yield of the implosion. While these improvements are underway, the 100-Gbar Campaign has a parallel effort using a statistical approach to search for the optimum DT cryogenic implosion on OMEGA having the highest combination of areal density and primary neutron yield using the current capabilities [19]. The MegaJoule Direct-Drive (MJDD) Campaign at the NIF investigates direct-drive physics at long-scale lengths [20-24]. The behavior especially of the laser plasma interactions (LPI) in coronal plasma characteristic of LDD ignition target designs is challenging to predict with certainty; therefore, experiments are conducted in plasma having the relevant temperature and scale length on NIF for LPI, as well as for laser coupling and laser imprint. The National Direct-Drive Program is a multi-year, systematic research effort with an overarching goal of understanding the physics of laser-direct-drive implosions.

The National Direct-Drive Program includes OMEGA and NIF experiments to study direct drive-target physics as shown in Fig. 1. Laser coupling, preheat, imprinting, and

hydrodynamically-scaled implosions from ignition designs for the NIF are investigated on OMEGA [19, 25-32]. The NIF laser direct-drive target has a diameter that is about four times the size of an OMEGA target and is driven with laser energy that is approximately seventy times larger than OMEGA. The NIF coronal plasmas have a longer density scale length and a higher electron temperature than the OMEGA coronal plasmas, which could affect laser coupling, preheat, and laser imprint. Modeling and simulations of laser coupling, preheat, and laser imprint are tested at the MJ scale with NIF direct-drive experiments to validate their accuracy [20-24].

Laser direct drive requires a hot-spot pressure above 120 Gbar and a convergence ratio above 22 to achieve ignition assuming an ion temperature of 4 keV [1-3, 25, 27]. Current α~3.5 (α is the ratio of the pressure in the compressed DT shell to the Fermi-degenerate pressure), DT cryogenic implosions on OMEGA achieve a hot-spot pressure of 56±7 Gbar and an energy-scaled Generalized Lawson Parameter [27] of 0.6 to 0.64 [30]. The hot-spot pressure ($P_{\rm hs}$) is an invariant metric with respect to laser energy; consequently, achieving 100 Gbar on OMEGA ensures that 100 Gbar would be achieved on the NIF assuming similar energy coupling at the two target scales. The ignition threshold pressure expressed as a function of the hot-spot thermal energy is $P_{\rm hs} > 250\ {\rm Gbar}/\sqrt{E_{\rm hs}/10\ {\rm kJ}}$ [1, 33]. Increasing laser coupling and $E_{\rm hs}$ reduces $P_{\rm hs}$ required for ignition. Symmetric direct-drive–ignition capsule designs on the NIF are predicted to couple up to 40 kJ to the hot spot, resulting in a required pressure of $P_{\rm hs}$ = 120 Gbar, which could be achieved in an implosion with a convergence ratio (CR) of 22, and an in-flight aspect ratio (IFAR)—defined as the shell radius divided by its thickness at maximum implosion velocity—of

24 if the energy coupling losses from CBET have been mitigated. Current OMEGA implosions [1-3, 27] reach E_{hs} = 0.44 kJ without any CBET mitigation. When scaled to 1.8 MJ of UV energy on the NIF with scaled CBET losses, these OMEGA implosions are predicted to reach $E_{hs} \approx 30$ kJ, increasing the required P_{hs} to 144 Gbar. With this E_{hs}, capsule designs with CR = 25 and an IFAR of 33 are required to reach the ignition conditions albeit with decreased robustness to hydrodynamic instabilities and low-mode drive asymmetries. When scaled to the laser energy available on NIF, the current DT cryogenic implosions on OMEGA achieve about 40% of the pressure required for ignition [1-3, 27]. Extensive analysis of the current α~3.5, DT cryogenic implosion experiments [27] and two- and three-dimensional simulations suggest that power balance, target offset, target quality, and CBET are the main limiting factors in target performance [1, 13, 14]. Because of the required E_{hs} for direct-drive ICF, the ignition-relevant P_{hs} and CR are lower than the requirements for laser indirect-drive (LID) ICF: P_{hs} = 350 to 400 Gbar and CR = 30 to 40 [34, 35]. Recently, laser indirect drive (LID) on NIF has demonstrated it is possible to achieve a hot-spot pressure of ~360 Gbar [36] that exceeds the requirements for LDD.

The physics goals and the laser and target requirements are derived from ignition target designs at the MJ energy scale. OMEGA implosions are hydrodynamically scaled from the NIF direct-drive ignition design (i.e,. radius~ laser energy$^{1/3}$, time ~ laser energy$^{1/3}$, and laser power ~ laser energy$^{2/3}$) as shown in Fig. 2 [25]. The target design parameters studied on OMEGA are as follows: the velocity of the imploding shell (V_{imp}) ranges from 3.5 to 5.0 x 10^7 cm/s; the adiabat in the compressed DT shell quantifying the ratio of the pressure to the Fermi-degenerate pressure ($\alpha = P / P_F$) is in the range of 2 to 7; the convergence ratio of the implosion (CR) is 10 to 23; and

the in-flight aspect ratio (IFAR) is 15 to 50 [1-3, 25, 27].

The National Direct-Drive ICF Program has four elements. The first element is the investigation of hydro-equivalent implosions on OMEGA involving a demonstration and physics understanding of ignition-relevant hot-spot pressure (100 Gbar), and an understanding and control of laser plasma interactions (LPI). This includes cross beam energy transfer (CBET) [1-3, 25, 28, 37-39], two-plasmon-decay instability (TPD) [18, 23, 40], and stimulated Raman scattering (SRS) [23, 41]. CBET reduces the coupling of laser energy to the imploding shell, and TPD and SRS are potential sources of suprathermal electrons that can cause the thermonuclear fuel to be preheated. The second element involves an investigation of LPI, energy coupling, and imprint mitigation at the MJ-scale on the NIF [20-24]. It includes planar, implosion, and cone-in-shell target platforms. The third element is to develop a strategy for conversion of NIF to spherical direct drive (SDD). Currently only polar-direct-drive [20] implosions can be performed on the NIF with the current beam configuration [5, 20-24]; however, spherical direct drive is the ultimate goal of the National Direct-Drive Program. A study was undertaken to review the cost, schedule, and phased approach to convert NIF from its current polar configuration of laser beams entering the NIF target chamber to a SDD configuration. It will involve laser technology development on NIF for LDD laser beam smoothing requirements. The fourth element is the development of robust target designs for a range of target performance extending from modest levels of alpha heating to low-energy gain [42]. The goal of the National Direct-Drive ICF Program is to determine the physics and laser requirements for multi-MJ direct-drive target performance.

An overview of the multi-year, systematic effort that is underway for the National

Direct-Drive Inertial Confinement Fusion Program, including laser, target, and diagnostic improvements that are in progress, as well as recent developments from the 100-Gbar Campaign on OMEGA and MJDD Campaign on NIF is presented in this paper. The 100-Gbar Campaign and the MJDD Campaign are described in Section II, which is followed by the conclusions.

II. 100-Gbar Campaign on OMEGA and MJDD Campaign on NIF

The 100-Gbar Campaign on OMEGA explores the formation of hot-spot conditions relevant for ignition at the MJ scale. Extensive analysis of the current α~3.5, DT cryogenic implosion experiments [27] and two- and three-dimensional simulations suggest that laser power balance, target offset, target quality, and CBET are the main limiting factors in target performance [1, 13, 14, 27]. Achieving an ignition-relevant hot-spot pressure on OMEGA involves the following critical research activities: improving laser power balance and the quantifying the overlapped intensity on target; developing a fill-tube target to field non-permeable ablators; mitigating laser plasma interactions (LPI) of CBET and TPD; developing laser upgrades for LPI mitigation; improving implosion modeling and simulation; optimizing the implosion yield and areal density; mitigating laser imprint; controlling the shock timing and adiabat; improving the physics models used in LDD hydrodynamics codes with high energy density physics (HEDP) experiments and first-principles computations; and the development of diagnostics for all phases of the implosion especially to understand multi-dimensional effects on stagnation. Many of the hot-spot diagnostics are developed in collaboration with the National Diagnostics Working Group [43].

The 100-Gbar Campaign has two approaches to increase the hot-spot pressure: the enhanced-capability and the statistical approach. The strategy of the enhanced-capability

approach of the 100-Gbar Campaign is highlighted in Fig. 3 showing the areal density plotted as a function of the primary neutron yield with the calculated contours of hot-spot pressure overlaid. It involves improvements to OMEGA laser [1-3], targets [8], diagnostics [9-12], and new modeling and simulation capabilities [13-18] to increase the areal density and yield of the implosion. These improvements will be applied to the α ~3.5 DT cryogenic implosion where the highest hot-spot pressure (56 ±7 Gbar) was achieved with an energy-scaled Generalized Lawson Parameter of 0.6 to 0.64 [27], which extrapolates to a 125-kJ of fusion yield on a symmetric NIF LDD implosion [30]. The goals will be to increase the hot spot pressure to 80 Gbar with an energy-scaled Generalized Lawson Parameter of 0.8 by 2020 and to increase further the hot-spot pressure above 100 Gbar with an energy-scaled Generalized Lawson Parameter of 0.95-0.98 by 2023. The enhanced-capability approach fixes long- and short-wavelength perturbations, mitigates LPI, and increases the energy coupling to increase yield and areal density by coupling more energy to a spherically-symmetric hot spot at stagnation.

The statistical approach highlighted in Fig. 4 is a parallel effort to the enhanced-capability approach. The objective is to develop a predictive capability based on a statistical approach to search for the optimum DT cryogenic implosion on OMEGA having the highest combination of areal density and primary neutron yield using the current capabilities [19]. The statistical approach varies the target dimensions (i.e., outside diameter of the target, wall thickness of the plastic ablator, and wall thickness of the DT ice layer) and adiabat to maximize target performance. The start point for the first path of the optimization campaign is a high-adiabat implosion (α ~5-7) with a low-convergence ratio (CR~10). A second path will be pursued in the

future with a starting point of a low-adiabat and high convergence ratio implosion. The experiments are guided by a new predictive tool that uses a statistical mapping of the measured yields onto the simulated implosion velocities and stagnated masses [19]. The laser energy coupling to the target increases as the target diameter increases as a result of higher laser absorption caused by an increasing density scale length and a reduction in CBET as the ratio of the radius of the beam to the radius of the target is less than unity [28]. The implosion velocity is increased further by reducing the payload. A yield of $1.17\pm0.06 \times 10^{14}$ and an areal density of 165 ± 23 mg/cm^2 was recorded corresponding to an energy-scaled Generalized Lawson Parameter of 0.7, which extrapolates to a ~300-kJ of fusion yield on a symmetric NIF LDD implosion [19]. The statistical approach will incorporate improvements to OMEGA targets, diagnostics, and modeling as they become available.

Improvements in targets are required for the 100 Gbar Campaign and ongoing research will refine these needs. The need for a DT cryogenic fill-tube target requirement for the 100-Gbar Campaign [44] is based on the following factors: non-permeable capsules are needed to optimize ablator and laser plasma instability mitigation [25]; target debris and defects seeding hydrodynamic instabilities need to be minimized; and the radiation damage to the ablator needs to be minimized. An example of a non-permeable, multilayer ablator target designed to mitigate laser imprint and the TPD [25] is shown in Fig. 5(a). The prototype fill-tube target for OMEGA [44] is shown in Fig. 5(b) with a 10-μm diameter fill tube supporting the capsule having an outside diameter of 860 μm.

The delivery of the DT to the interior volume of the spherical shell plastic ablator via fill tube

substantially reduces the radiation damage to the capsule from the beta decay of the tritium compared to the high-pressure DT permeation fill technique [45]. The current DT cryogenic implosion targets are filled on OMEGA via permeation [45]: An OMEGA cryogenic target is ~1 mm-diameter spherical shell having a wall thickness of ~8-μm, and supported by a SiC stalk having a 17-μm diameter. Five targets are placed in a pressure vessel surrounded by a cryostat. The pressure is increased linearly in the vessel with slow pressure ramp (~0.7 atm/min) up to a maximum pressure of 1500 atm. to allow the gas to permeate through the shell wall without buckling the shells, while the temperature is maintained at 300 K throughout the pressurization cycle to allow rapid gas permeation. The targets are cooled at a slow rate (~0.1 K/min) to 26 K once the peak pressure is reached. At this temperature, both the shell and pressure vessel contain liquid DT with a vapor pressure of a few atm. and the plastic shell is no longer permeable. Gas outside of the shell is recovered, while the gas inside the shell is trapped and has too low a pressure to burst the shell. During the high-pressure DT permeation fill the plastic ablator is exposed to the beta decay of the tritium, which breaks the chemical bonds in the plastic. Although the range of the beta particle in plastic is short (<1 μm) relative to the thickness of the plastic ablator (8 μm), the high-pressure DT permeation process exposes the entire plastic shell (i.e., inner wall, outer wall, and bulk) to radiation damage. The dose is estimated to exceed 200 MRad. The DT comprising the layer within the plastic shell exposes the inner wall of the shell to radiation from beta decay at a rate of 4 MRad/hour. In contrast to the targets filled via high-pressure DT permeation, the radiation damage to the fill-tube target from the beta decay of tritium is substantially lower and is restricted to the inner wall of the plastic ablator at a rate of 4

MRad/hour. The fill-tube DT cryogenic target will be fielded on OMEGA in 2020 [44].

Polystyrene (PS) capsules and polished glow discharge polymer (GDP) capsules are being developed to minimize target debris and defects [3], which seed hydrodynamic instabilities [46]. In Fig. 6(a) the defects on the surface of a GDP capsule measured using atomic force microscopy are shown. In Fig. 6(b) and Fig. 6(c) the heights of the surface defects are compared to the lateral dimensions or defect sizes for a sample area representing a few percent of the total surface area of the capsule. The black curve in each plot represents the tolerable level of defects base on LDD hydrodynamic simulations [46]. A limited number of defects above the black curve is predicted to be tolerable for the 100 Gbar goal [3]. A comparison of Fig. 6(b) with Fig. 6(c) reveals the PS capsule has a superior surface quality to the GDP one. PS capsules are being developed to achieve the 80-Gbar goal [3]. Hydrodynamic mixing of the ablator into the hot spot of DT cryogenic implosions is diagnosed on OMEGA with Ge K-shell spectroscopy [3], using a technique developed on NIF [47-49]. Laser imprint could also seed hot-spot mix. Controlled experiments will be conducted to determine the contributions to hydrodynamic mixing seeded by surface debris and defects, engineering features like the fill tube or stalk, and laser imprint. Mitigation strategies for laser imprint using high-Z overcoat layers [50] are being investigated on OMEGA using laser and x-ray pre-pulse to expand the Au layer in advance of the laser-drive pulse. Low-density foams of low-/mid-Z materials are being explored to mitigate laser imprint for LDD: for foam densities above the critical density of the drive laser, the mechanism of laser-imprint mitigation relies on the reduced growth rate of Rayleigh-Taylor instability, due to the increased ablation velocity and density-scale-length at the ablation surface

[51].

The system requirements for the 80-Gbar goal are an on-target, overlapped laser intensity of 1% rms, corresponding to a beam-to-beam intensity balance of 3% rms averaged over 100 ps, a target placement accuracy of less than 10 μm, and PS ablators. The targets will be filled using the high-pressure DT permeation fill station [45], which positions 80% of the targets within 15 μm of the desired location as shown in Fig. 7(a). The hard-sphere calculation of the overlapped laser intensity on an OMEGA DT cryogenic implosion target having a 20-μm offset is shown in Fig. 7(b) to result in a 10% diametric imbalance in the laser drive. CBET mitigation using spatial technique of reducing the radius of the beam to the initial radius of the target (R_{beam}/R_{target} = 0.75) using a specially designed phase plate will be implemented [16] for the 80-Gbar goal. Laser upgrade research for LPI mitigation will proceed in parallel, along with the development of multilayered ablators (CH/Si/CHSi) for TPD control. TPD control will become more important as CBET is mitigated and the intensity at the quarter-critical density increases.

OMEGA gains, losses, frequency conversion, near fields, and far fields are being diagnosed and balanced amongst the 60 beams to reduce the on-target, laser-drive nonuniformity. In Fig. 8(a) the rms imbalance in the 60 OMEGA beams during the picket portion of the laser drive is plotted for the last few years. It shows a steady decline from 6% down to 2%. However, as shown in Fig. 8(b), these measurements are performed just after the frequency conversion crystals and not inside of the target chamber where they are required. On-target ultraviolet (UV) and x-ray imaging diagnostics are being developed to diagnose the on-target, overlapped intensity. Direct measurements will eliminate any assumptions associated with diagnosing the on-target

intensity using equivalent target plane diagnostics. Proof-of-principle experiments using implosions of gas-filled plastic shell targets demonstrated subpercent-scale control of low modes at a convergence ratio of three with 3-D gated x-ray imaging [12]. This target-physics experimental technique provides an independent check on the direct measuremnts of the laser drive. 3-D effects of the laser-drive nonuniformity will be diagnosed next for DT cryogenic implosions.

Laser plasma interactions (CBET, TPD, SRS) are being investigated on OMEGA and NIF [23, 24]. A spatial technique to mitigate CBET has been demonstrated on OMEGA by reducing the ratio of the radius of the beam to the initial target radius [28, 37-39]. A 40% increase in the hydrodynamic efficiency, defined as the ratio of the shell kinetic energy to the laser energy incident on the target, was observed due to a reduction in CBET when the initial target diameter was increased from 800 to 1000 μm, while keeping the laser beam diameter fixed at 825 μm [28]. The first observation of CBET mitigation for LDD implosions using wavelength detuning was demonstrated in proof-of-principle experiments at the NIF [24]. The suprathermal electron generation by LPI (SRS, TPD) in ignition-scale coronal plasmas was examined on NIF, and the estimated fraction of laser energy in hot electrons was found to be close to tolerable levels for LDD ignition designs [23]. Follow-on experiments are planned to examine the amount of hot electron energy that is deposited in the imploding shell. As shown in Fig. 9 an OMEGA EP beam having a tunable optical parametric amplifier capable of operating in the 350.2 to 353.4 nm wavelength range is being transported to the OMEGA target chamber and will propagate along the P9 axis for LPI experiments. The beam is called the tunable OMEGA P9 beam or TOP9.

Fundamental CBET experiments crossing the TOP9 beam with other OMEGA beams in a gas-jet plasma are planned first, followed by TPD experiments using the TOP9 beam, and integrated implosion experiments. The objective is to use the TOP9 beam to define the requirements for future LPI mitigation on OMEGA.

Accurate knowledge of DT and ablator properties, such as equation of state (EOS) [52-58], opacity [59, 60], conductivity [61, 62], and stopping power of charged particles for high energy density physics, is required for LDD simulations. The microphysics models used in hydrodynamics codes are being improved through experiments and first-principles computations. Focused experiments are being conducted to study shock timing, coalescence, breakout, and hydrodynamic mixing at interfaces.

Three-dimensional (3-D) diagnostics (i.e., more than three diagnostic lines of sight (LOS)) are being developed to study multi-dimensional effects on the hot-spot at stagnation [9-12]. X-ray [9] and nuclear [10, 11, 32] diagnostics are being developed to study hot-spot formation and stagnation. 3-D gated x-ray imaging of the hot spot formation and disassembly with less than 5-μm spatial, ~10-ps temporal resolution is being developed [9]. The neutron spectrum will be diagnosed with the neutron time of flight detectors along multiple LOS to infer the hot-spot ion temperature, the compressed areal density of the DT shell, spatial variations in these quantities, the fusion yields, and evidence of residual flows in the hot spot [10, 11, 32]. Developing brighter x-ray sources and higher spatial resolution x-ray imagers is underway to probe the compressed fuel layer using 1.86-keV x-ray backlighting at stagnation [63]. Absolute time- and space-resolved hot-spot X-ray continuum diagnostics to infer the electron temperature of the hot

spot, the compressed areal density of the DT shell, and the hot-spot mix mass are under development and will be extended to multiple LOS. 3-D diagnostics will provide experimental insights to understand the multi-dimensional effects.

IV. CONCLUSION

The strategy of the National Direct-Drive Inertial Confinement Fusion Program consisting of the 100-Gbar Campaign on the 30-kJ, 351-nm, 60-beam OMEGA Laser System and the MegaJoule Direct Drive (MJDD) Campaign on the 1.8-MJ, 351-nm, 192-beam National Ignition Facility (NIF) was presented. Progress achieving the main goals of the 100-Gbar Campaign to demonstrate and understand the physics for hot-spot conditions and formation relevant for ignition at the MJ scale, and the MJDD Campaign to understand the laser plasma interactions, energy coupling, and laser imprint for ignition-scale direct-drive coronal plasmas was reported. Extensive analysis of the current α~3.5, DT cryogenic implosion experiments and two- and three-dimensional simulations suggest that laser power balance, target offset, target quality, and CBET are the main limiting factors in target performance. Achieving an ignition-relevant hot-spot pressure on OMEGA involves the following critical research activities: improving laser power balance and the quantifying the overlapped intensity on target; developing a fill-tube target to field non-permeable ablators; mitigating LPI of CBET and TPD; developing laser upgrades for LPI mitigation; improving implosion modeling and simulation; optimizing the implosion yield and areal density using the statistical approach; mitigating laser imprint; controlling the shock timing and adiabat; improving the physics models used in LDD hydrodynamics codes with high

energy density physics (HEDP) experiments and first-principles computations; and the development of diagnostics for all phases of the implosion especially to understand the multi-dimensional effects on stagnation. The behavior especially of the laser plasma interactions (LPI) in coronal plasma characteristic of LDD ignition target designs is challenging to predict with certainty; therefore, experiments are conducted in plasma having the relevant temperature and scale length on NIF for LPI, as well as for laser coupling and laser imprint to validate the predictions.

VI. ACKNOWLEDGMENTS

The authors acknowledge the outstanding operation of the OMEGA laser system and the National Ignition Facility. This material is based upon work supported by the Department Of Energy National Nuclear Security Administration under Award Number DE-NA0001944, Lawrence Livermore National Laboratory under Contract DE-AC52-07NA27344, the University of Rochester, and the New York State Energy Research and Development Authority. The support of DOE does not constitute an endorsement by DOE of the views expressed in the article.

REFERENCES

[1] V. N. GONCHAROV et al., "National Direct-Drive Program on OMEGA and the National Ignition Facility," Plasma Phys. Control. Fusion, **59**, 1, 014008 (2017); https://doi.org/10.1088/0741-3335/59/1/014008.

[2] E. M. Campbell et al., "Laser-direct-drive program: Promise, challenge, and path forward," Matter and Radiation at Extremes 2, 37 (2017).

[3] S. P. Regan et al., "The National Direct-Drive Program: OMEGA to the National Ignition Facility," Fusion Science and Technology **73**, 89 (2018); https://doi.org/10.1080/15361055.2017.1397487

[4] T. R. BOEHLY et al., "Initial Performance Results of the OMEGA Laser System," *Opt. Commun.*, **133**, *1–6*, 495 (1997); https://doi.org/10.1016/S0030-4018(96)00325-2.

[5] E. M. CAMPBELL and W. J. HOGAN, "The National Ignition Facility—Applications for Inertial Fusion Energy and High-Energy-Density Science," *Plasma Phys. Control. Fusion*, **41**, *12B*, B39 (1999); https://doi.org/10.1088/0741-3335/41/12B/303.

[6] R. S. CRAXTON et al., "Direct-Drive Inertial Confinement Fusion: A Review," *Phys. Plasmas*, **22**, *11*, 110501 (2015); http://dx.doi.org/10.1063/1.4934714.

[7] D. H. Crandall, "The quest for laboratory inertial fusion burn in the United States," Journal of Physics: Conference Series 717, 012001 (2016); doi:10.1088/1742-6596/717/1/012001.

[8] D. R. Harding et al., "Requirements and Capabilities for Fielding Cryogenic DT-Containing Fill-Tube Targets for Direct-Drive Experiments on OMEGA," Fusion Science and Technology

73, 324 (2018); https://doi.org/10.1080/15361055.2017.1374812

[9] W. Theobald et al., "The Single Line-of-Sight Time-Resolved X-ray Imager diagnostic on OMEGA," Rev. Sci. Instrum., (in print);

[10] O. Mannion et al., "Calibration of a neutron time-of-ight detector with a rapid instrument response function for measurements of bulk uid motion on OMEGA," Rev. Sci. Instrum. (in print).

[11] V. Glebov et al., "Testing a Cherenkov Neutron Time-of-Flight Detector on OMEGA," Rev. Sci. Instrum. (in print).

[12] D. T. Michel et al., "Subpercent-scale control of 3D low modes of targets imploded in direct-drive configuration on OMEGA," Phys. Rev. Lett. 120, 125001 (2018).

[13] I. V. Igumenshchev *et al*., Phys. Plasmas **23**, 052702 (2016).

[14] I. V. Igumenshchev *et al*., Phys. Plasmas **24**, 056307 (2017).

[15] S. X. Hu et al., Phya. Plasmas 25, 056306 (2018).

[16] S. X. Hu et al., this issue of Nuclear Fusion

[17] J. F. Myatt et al., Phys. Plasmas 24, 056308 (2017).

[18] R. K. Follett et al., Phys. Rev. Lett 120, 135005 (2018).

[19] V. Gopalaswamy et al., "," submitted to Nature Physics.

[20] S. SKUPSKY et al., "Polar Direct Drive on the National Ignition Facility," *Phys. Plasmas*, **11**, *5*, 2763 (2004); http://dx.doi.org/10.1063/1.1689665.

[21] M. HOHENBERGER et al., "Polar-Direct-Drive Experiments on the National Ignition Facility," *Phys. Plasmas*, **22**, *5*, 056308 (2015); http://dx.doi.org/10.1063/1.4920958.

[22] P. B. Radha et al., "Direct drive: Simulations and results from the National Ignition Facility," Physics of Plasmas **23**, 056305 (2016); doi: 10.1063/1.4946023

[23] M. J. Rosenberg et al., "Origins and Scaling of Hot-Electron Preheat in Ignition-Scale Direct-Drive Inertial Confinement Fusion Experiments," Phys. Rev. Lett. **120**, 055001 (2018); doi: 10.1103/PhysRevLett.120.055001.

[24] J. A. Marozas et al., "First Observation of Cross-Beam Energy Transfer Mitigation for Direct-Drive Inertial Confinement Fusion Implosions Using Wavelength Detuning at the National Ignition Facility," Phys. Rev. Lett. 120, 085001 (2018); DOI: 10.1103/PhysRevLett.120.085001

[25] V. N. GONCHAROV et al., "Improving the Hot-Spot Pressure and Demonstrating Ignition Hydrodynamic Equivalence in Cryogenic Deuterium–Tritium Implosions on OMEGA," *Phys. Plasmas*, **21**, *5*, 056315 (2014); http://dx.doi.org/10.1063/1.4876618.

[26] R. Betti, A. R. Christopherson, B. K. Spears, R. Nora, A. Bose, J. Howard, K. M. Woo, M. J. Edwards, and J. Sanz, Phys. Rev. Lett. 114, 255003 (2015).

[27] S. P. REGAN et al., "Demonstration of Fuel Hot-Spot Pressure in Excess of 50 Gbar for Direct-Drive, Layered Deuterium-Tritium Implosions on OMEGA," Phys. Rev. Lett. **117** (2), 025001 (2016); **117** (5), 059903(E) (2016); http://doi.org/10.1103/PhysRevLett.117.025001.

[28] S. P. Regan et al., "Energy Coupling and Hot-Spot Pressure in Direct-Drive Layered Deuterium-Tritium Implosions on OMEGA," submitted to Physics of Plasmas (2018).

[29] V. N. GONCHAROV et al., "Demonstrating Ignition Hydrodynamic Equivalence in Direct-Drive Cryogenic Implosions on OMEGA," *J. Phys.: Conf. Ser.*, **717**, 012008 (2016); https://doi.org/10.1088/1742-6596/717/1/012008.

[30] A. Bose et al., "Core conditions for alpha heating attained in direct-drive inertial confinement fusion," Phys. Rev. E 94, 011201(R) (2016); DOI: 10.1103/PhysRevE.94.011201

[31] A. Bose et al., "Analysis of trends in experimental observables: Reconstruction of the implosion dynamics and implications for fusion yield extrapolation for direct-drive cryogenic targets on OMEGA Physics of Plasmas 25, 062701 (2018); https://doi.org/10.1063/1.5026780

[32] C. Forrest et al., "First Measurements of Deuterium-Tritium and Deuterium-Deuterium Fusion Reaction Yields in Ignition-Scalable Direct-Drive Implosions," Phys. Rev. Lett. **118**, 095002 (2017).

[33] V. N. GONCHAROV et al., "Demonstrating Ignition Hydrodynamic Equivalence in Direct-Drive Cryogenic Implosions on OMEGA," J. Phys.: Conf. Ser., 717, 012008 (2016); https://doi.org/10.1088/1742-6596/717/1/012008.

[34] O. A. HURRICANE et al., "Fuel Gain Exceeding Unity in an Inertially Confined Fusion Implosion," Nature, 506, 7488, 343 (2014); http://www.nature.com/nature/journal/v506/n7488/full/nature13008.html.

[35] T. DÖPPNER et al., "Demonstration of High Performance in Layered Deuterium-Tritium Capsule Implosions in Uranium Hohlraums at the National Ignition Facility," Phys. Rev. Lett., 115, 5, 055001 (2015); https://doi.org/10.1103/PhysRevLett.115.055001.

[36] S. Le Pape et al., "Fusion Energy Output Greater than the Kinetic Energy of an Imploding Shell at the National Ignition Facility," Phys. Rev. Lett. 120, 225003 (2018).

[37] I. V. IGUMENSHCHEV et al., "Crossed-Beam Energy Transfer in Implosion Experiments on OMEGA," *Phys. Plasmas*, **17**, *12*, 122708 (2010); http://dx.doi.org/10.1063/1.3532817.

[38] I. V. IGUMENSHCHEV et al., "Crossed-Beam Energy Transfer in Direct-Drive Implosions," *Phys. Plasmas*, **19**, *5*, 056314 (2012); http://dx.doi.org/10.1063/1.4718594.

[39] D. H. FROULA et al., "Increasing Hydrodynamic Efficiency by Reducing Cross-Beam Energy Transfer in Direct-Drive Implosion Experiments," *Phys. Rev. Lett.*, **108**, *12*, 125003 (2012); https://doi.org/10.1103/PhysRevLett.108.125003.

[40] C. Stoeckl, R. E. Bahr, B. Yaakobi, W. Seka, S. P. Regan, R. S. Craxton, J. A. Delettrez, R.W. Short, J. Myatt, A.V. Maximov, and H. Baldis, Phys. Rev. Lett. 90, 235002 (2003).

[41] W. L. KRUER, *The Physics of Laser Plasma Interactions*, Frontiers in Physics, Vol. 73, edited by D. PINES (Addison-Wesley, Redwood City, CA, 1988).

[42] T. J. B. Collins and J. A. Marozas, "Mitigation of cross-beam energy transfer in ignition-scale polar-direct-drive target designs for the National Ignition Facility," Physics of Plasmas (in print).

[43] *2016 Inertial Confinement Fusion Program Framework*, National Nuclear Security Administration, DOE/NA-044, p. 39 May (2016).

[44] D. R. HARDING et al., "Requirements and Capabilities for Fielding Cryogenic DT-Containing Fill-Tube Targets for Direct-Drive Experiments on OMEGA," Fusion Sci. Technol., 73, 3, 324 (2018); https://doi.org/10.1080/15361055.2017.1374812.

[45] D. R. HARDING et al., "Producing Cryogenic Deuterium Targets for Experiments on OMEGA," Fusion Sci. Technol., 48, 3, 1299 (2005); https://doi.org/10.13182/FST05-A1079.

[46] I. V. IGUMENSHCHEV et al., "Effects of Local Defect Growth in Direct-Drive Cryogenic Implosions on OMEGA," Phys. Plasmas, 20, 8, 082703 (2013);

http://dx.doi.org/10.1063/1.4818280.

[47] B. A. HAMMEL et al., "Diagnosing and Controlling Mix in National Ignition Facility Implosion Experiments," Phys. Plasmas, 18, 5, 056310 (2011); http://dx.doi.org/10.1063/1.3567520.

[48] S. P. REGAN et al., "Hot-Spot Mix in Ignition-Scale Implosions on the NIF," Phys. Plasmas, 19, 5, 056307 (2012); http://dx.doi.org/10.1063/1.3694057.

[49] S. P. REGAN et al., "Hot-Spot Mix in Ignition-Scale Inertial Confinement Fusion Targets," Phys. Rev. Lett., 111, 4, 045001 (2013); https://doi .org/10.1103/ PhysRevLett.111.045001.

[50] S. P. Obenschain et al., "Effects of thin high-Z layers on the hydrodynamics of laser-accelerated plastic targets," Phys. Plasmas 9, 2234 (2002).

[51] S. X. Hu et al., "Mitigating laser-imprint effects in direct-drive inertial-con_nement fusion implosions with an above-critical-density foam layer," submitted to Physics of Plasmas (2018).

[52] S. X. Hu et al., Phys. Rev. E 92, 043104 (2015).

[53] M. A. Barrios et al., Phys. Plasmas 17, 056307 (2010).

[54] M. A. Barrios et al., J. of Appl. Phys. 111, 093515 (2012).

[55] S. X. Hu et al., Phys. Rev. Lett. 104, 235003 (2010).

[56] S. X. Hu et al., Phys. Rev. B 84, 224109 (2011).

[57] T. R. Boehly et al., Phys. Plasmas 18, 092706 (2011).

[58] T. R. Boehly et al., Phys. Plasmas 11, L49 (2004).

[59] S. X. Hu et al., Phys. Rev. B 96, 144203 (2017).

[60] S. X. Hu et al., Phys. Rev. E 90, 033111 (2014).

[61] S. X. Hu et al., Phys. Plasmas 23, 042704 (2016).

[62] S. X. Hu et al., Phys. Rev. E 89, 043105 (2014).

[63] C. Stoeckl, Phys. Plasmas 24, 056304 (2017).

Figure Captions

Fig. 1. The OMEGA and NIF laser systems and schematics of LDD targets.

Fig. 2. The LDD ignition target design, laser power, and temporal evolution of the areal density for NIF (left panel), the hydrodynamically-scaled design for OMEGA, laser power, and temporal evolution of the areal density (right panel), and target design parameters (center panel).

Fig. 3. The strategy of the enhanced-capability approach is highlighted in the plot of the areal density versus primary neutron yield with hot-spot pressure contours overlaid.

Fig. 4. The strategy of the statistical approach to find the optimum implosion for OMEGA having the highest combination of yield and areal density.

Fig. 5. (a) schematic of multilayer target designed to mitigate laser imprint and TPD. (b) image of prototype fill-tube target for OMEGA.

Fig. 6. (a) Image of surface defects on GDP capsule characterized using atomic force microscopy. (b) Defect size and height for GDP ablator measurements taken on a few percent of the capsule surface is compared with LDD specification based on hydrodynamic simulations. A limited number of features above the black curve are acceptable. (c) Defect size and height for PS ablator measurements taken on a few percent of the capsule surface is compared with LDD specification based on hydrodynamic simulations. A limited number of features above the black curve are acceptable.

Fig. 7. (a) the percentage of DT cryogenic targets (filled via permeation) positioned a distance from the desired location at target chamber center (TCC). (b) a hard-sphere calculation of the overlapped laser intensity on an OMEGA implosion target assuming the target is mis-positioned

20 μm to the right.

Fig. 8. The measured improvement in the picket-energy balance over a few years period. (b) schematic of OMEGA laser bay and target bay highlighting location of current measurement for laser power balance and requirement to measure the on-target, overlapped laser intensity.

Fig. 9. Schematic of the OMEGA and OMEGA EP laser systems highlighting the TOP9 beam that will be used for LPI experiments on OMEGA.

Fig. 1

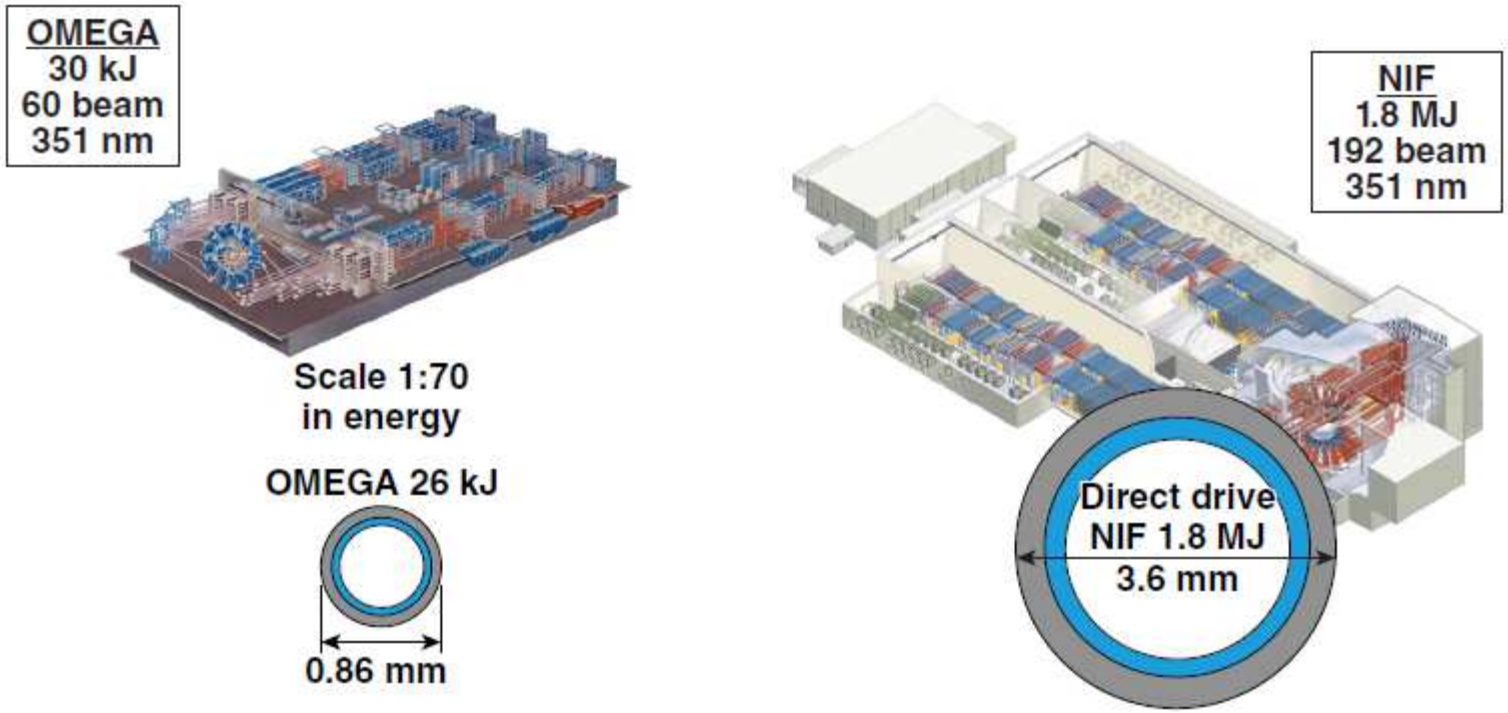
OMEGA
30 kJ
60 beam
351 nm
Scale 1:70
in energy
OMEGA 26 kJ
0.86 mm
NIF
1.8 MJ
192 beam
351 nm
Direct drive
NIF 1.8 MJ
3.6 mm

Fig. 2

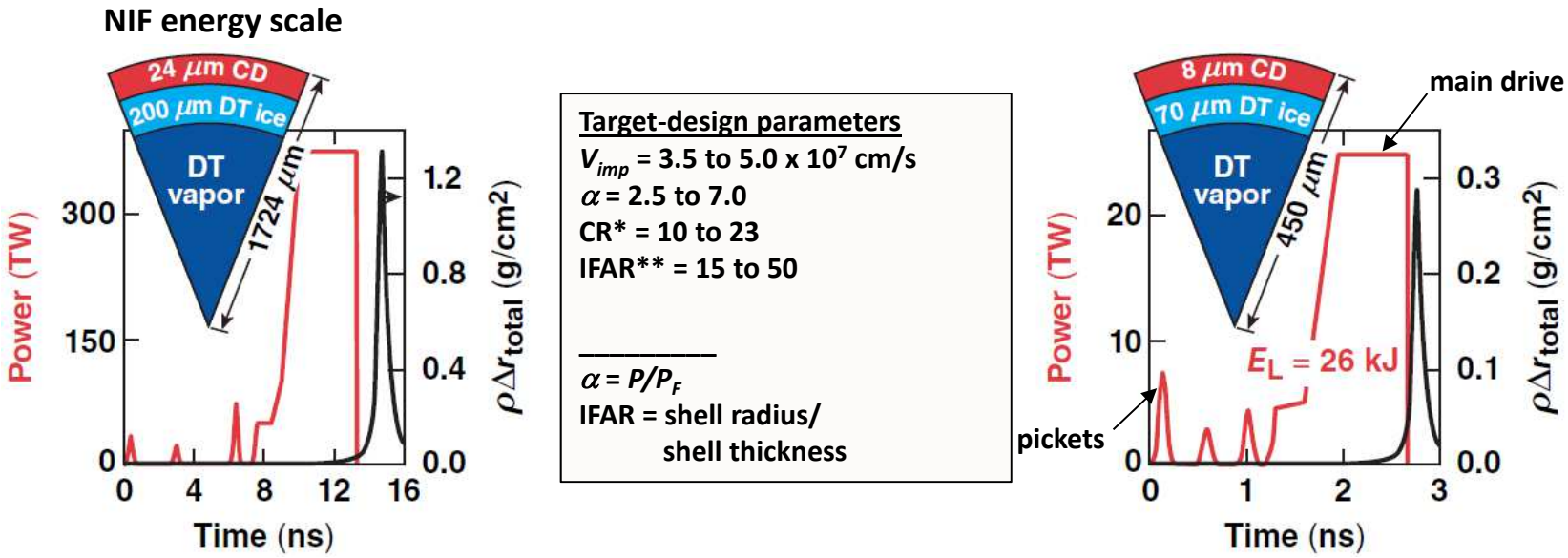
NIF energy scale
24 μm CD
200 μm DT ice
DT vapor
1724 μm
Power (TW)
300
150
0
0
4
8
12
16
Time (ns)
1.2
0.8
0.4
0.0
ρΔr_total (g/cm²)
Target-design parameters
V_imp = 3.5 to 5.0 x 10^7 cm/s
α = 2.5 to 7.0
CR* = 10 to 23
IFAR** = 15 to 50
α = P/P_F
IFAR = shell radius/ shell thickness
8 μm CD
70 μm DT ice
DT vapor
450 μm
main drive
E_L = 26 kJ
pickets
Power (TW)
20
10
0
0
1
2
3
Time (ns)
0.3
0.2
0.1
0.0
ρΔr_total (g/cm²)

Fig. 3

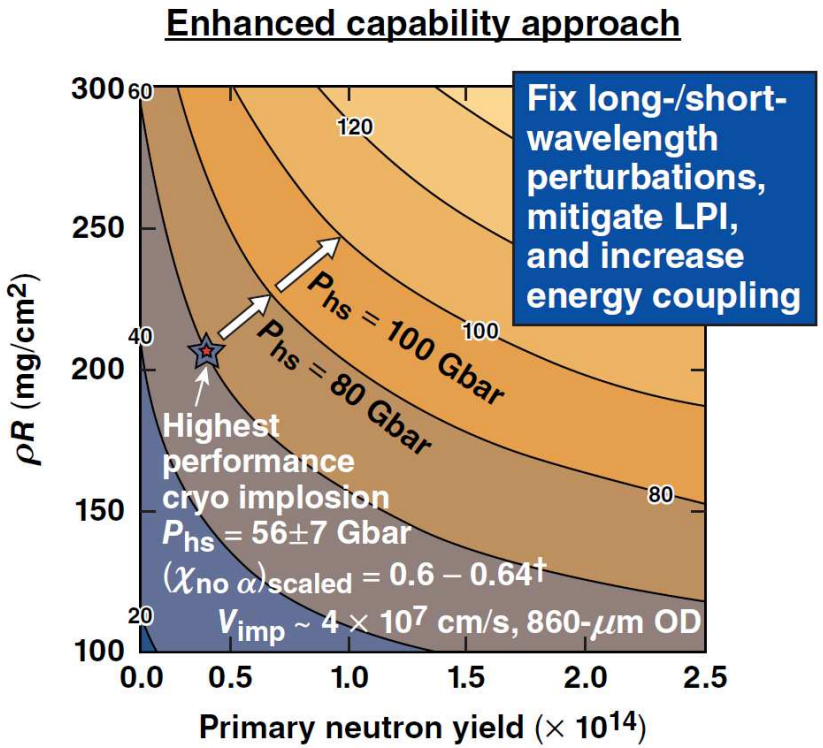
Enhanced capability approach
Fix long-/short-wavelength perturbations, mitigate LPI, and increase energy coupling
P_{hs} = 100 Gbar
P_{hs} = 80 Gbar
Highest performance cryo implosion
P_{hs} = 56±7 Gbar
$(\chi_{no\ \alpha})_{scaled}$ = 0.6 – 0.64†
V_{imp} ~ 4 × 10^7 cm/s, 860-μm OD
60
120
100
80
40
20
300
250
200
150
100
0.0
0.5
1.0
1.5
2.0
2.5
ρR (mg/cm^2)
Primary neutron yield (× 10^{14})

Fig. 4

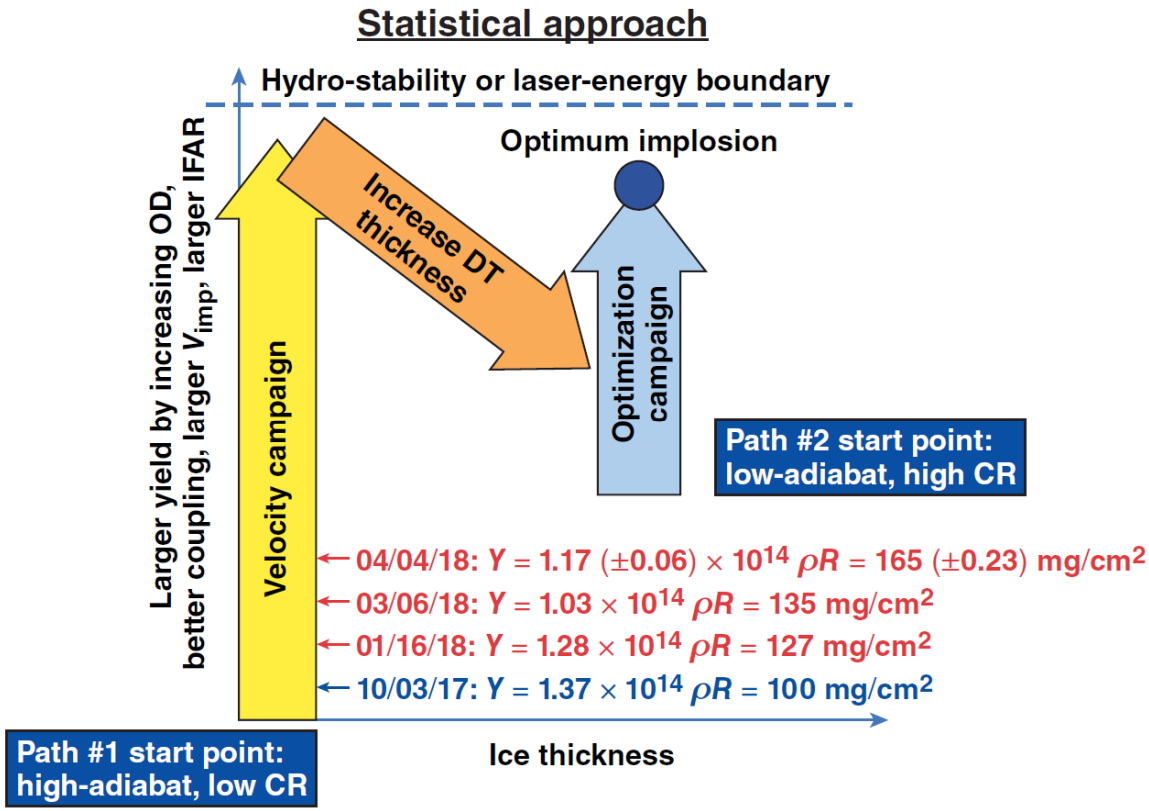
Statistical approach
Hydro-stability or laser-energy boundary
Optimum implosion
Increase DT thickness
Optimization campaign
Velocity campaign
Larger yield by increasing OD, better coupling, larger V_{imp}, larger IFAR
Path #2 start point: low-adiabat, high CR
04/04/18: $Y = 1.17\ (\pm 0.06) \times 10^{14}$ $\rho R = 165\ (\pm 0.23)$ mg/cm^2
03/06/18: $Y = 1.03 \times 10^{14}$ $\rho R = 135$ mg/cm^2
01/16/18: $Y = 1.28 \times 10^{14}$ $\rho R = 127$ mg/cm^2
10/03/17: $Y = 1.37 \times 10^{14}$ $\rho R = 100$ mg/cm^2
Path #1 start point: high-adiabat, low CR
Ice thickness

Fig. 5

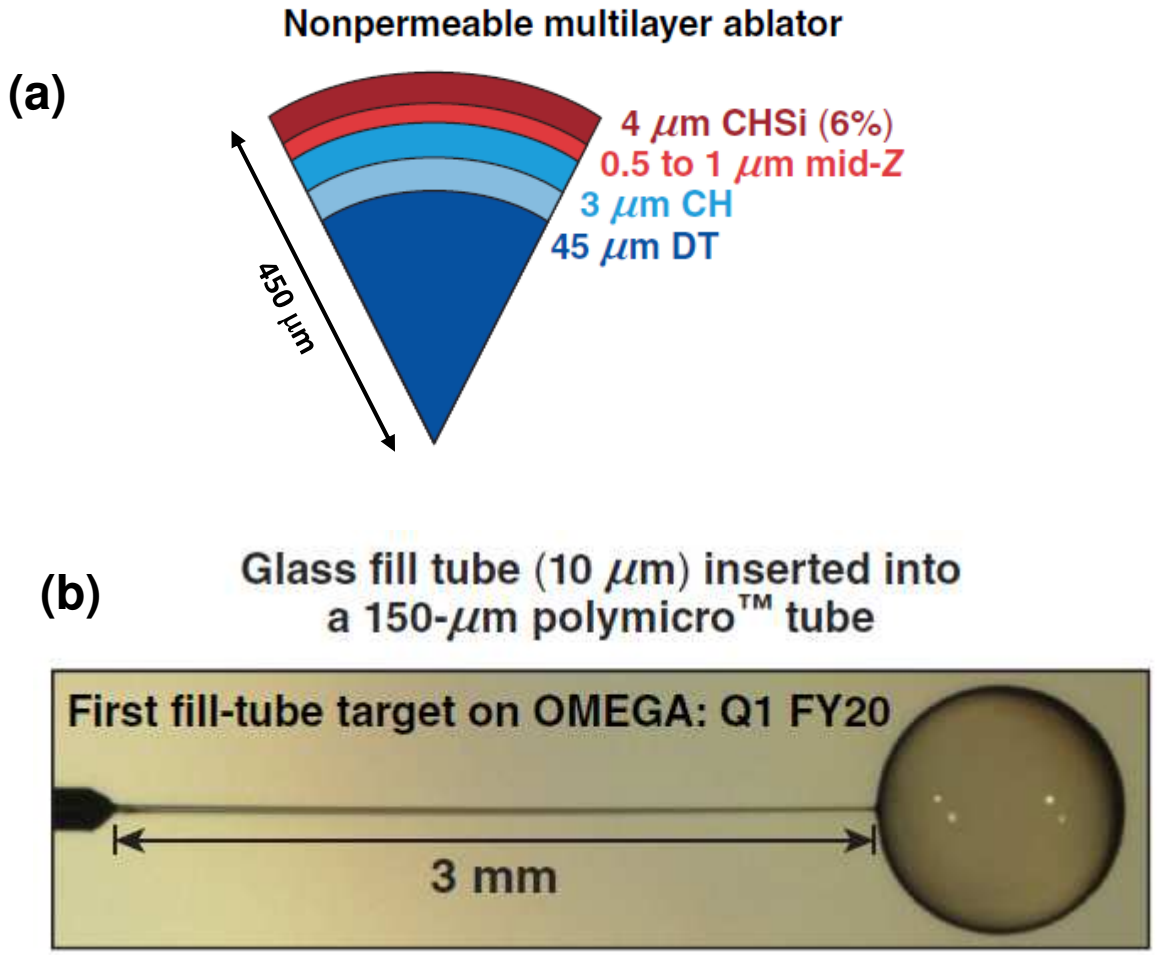
(a)
Nonpermeable multilayer ablator
4 μm CHSi (6%)
0.5 to 1 μm mid-Z
3 μm CH
45 μm DT
450 μm
(b)
Glass fill tube (10 μm) inserted into
a 150-μm polymicro™ tube
First fill-tube target on OMEGA: Q1 FY20
3 mm

Fig. 6

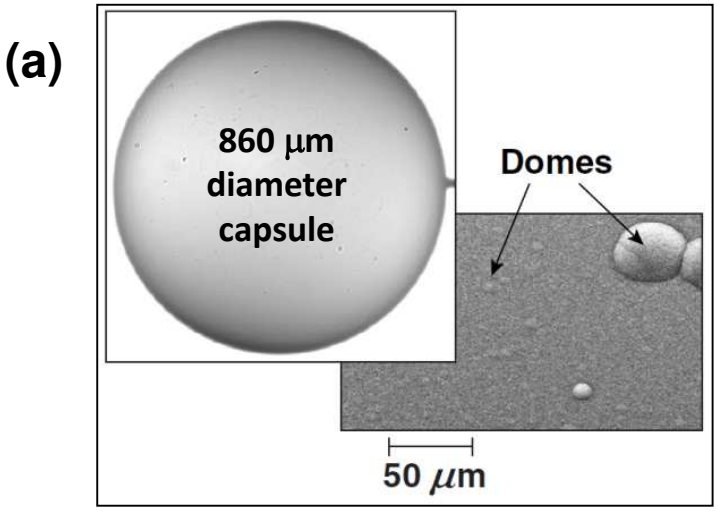
(a)
860 μm diameter capsule
Domes
50 μm

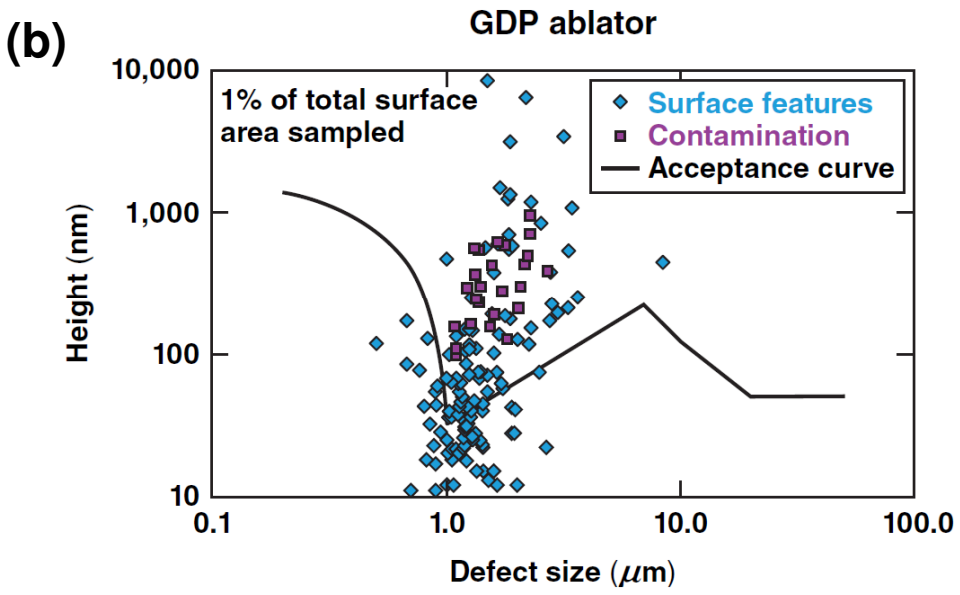
(b)
GDP ablator
1% of total surface area sampled
Surface features
Contamination
Acceptance curve
Height (nm)
10,000
1,000
100
10
0.1
1.0
10.0
100.0
Defect size (μm)

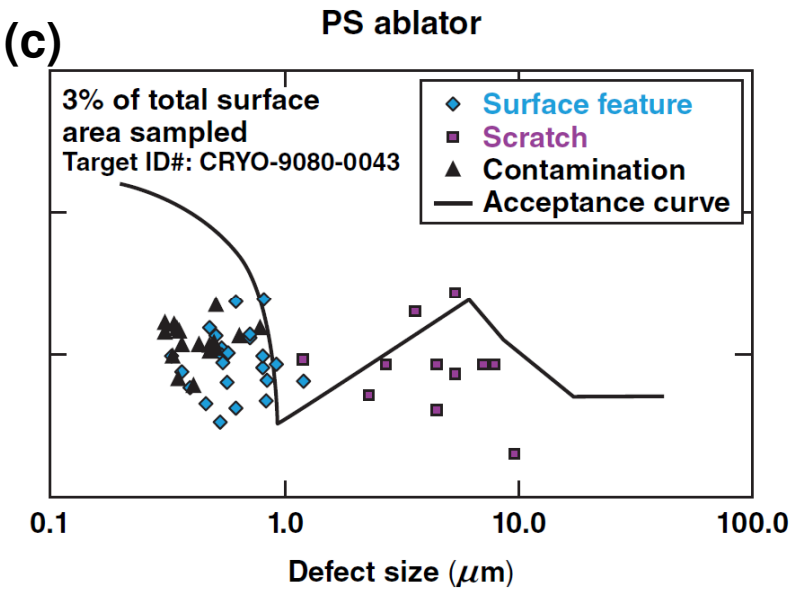
(c)
PS ablator
3% of total surface area sampled
Target ID#: CRYO-9080-0043
Surface feature
Scratch
Contamination
Acceptance curve
0.1
1.0
10.0
100.0
Defect size (μm)

Fig. 7

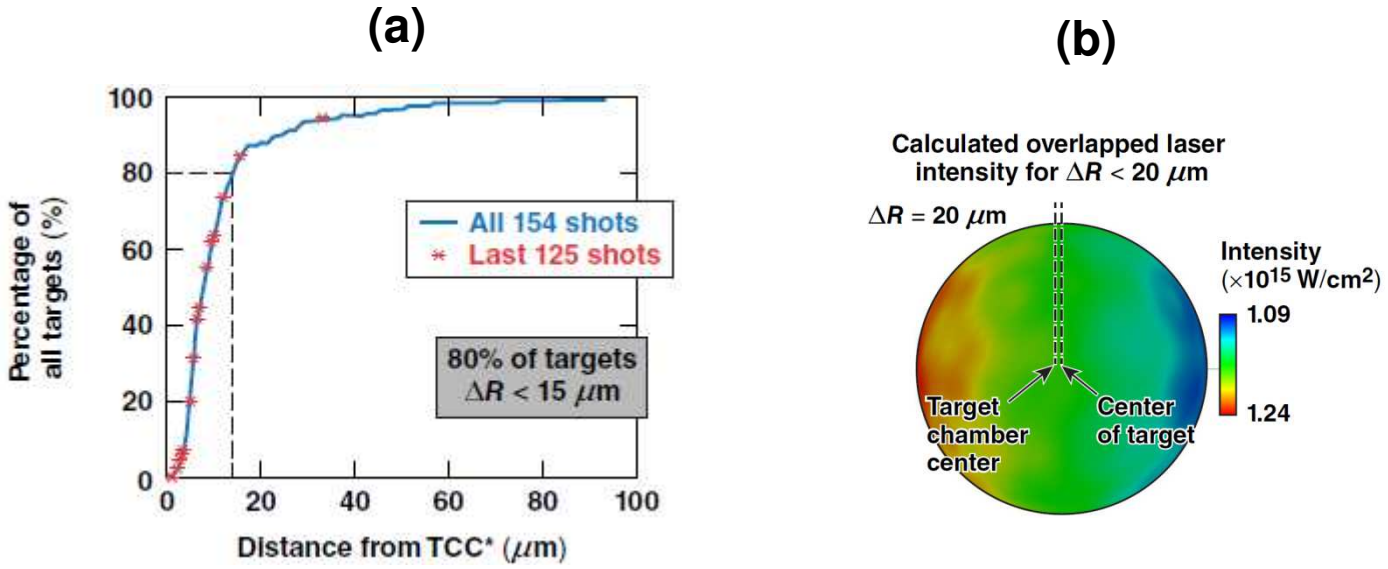
(a)
Percentage of all targets (%)
100
80
60
40
20
0
0
20
40
60
80
100
Distance from TCC* (μm)
All 154 shots
Last 125 shots
80% of targets
ΔR < 15 μm
(b)
Calculated overlapped laser intensity for ΔR < 20 μm
ΔR = 20 μm
Intensity
(×10^15 W/cm^2)
1.09
1.24
Target chamber center
Center of target

Fig. 8

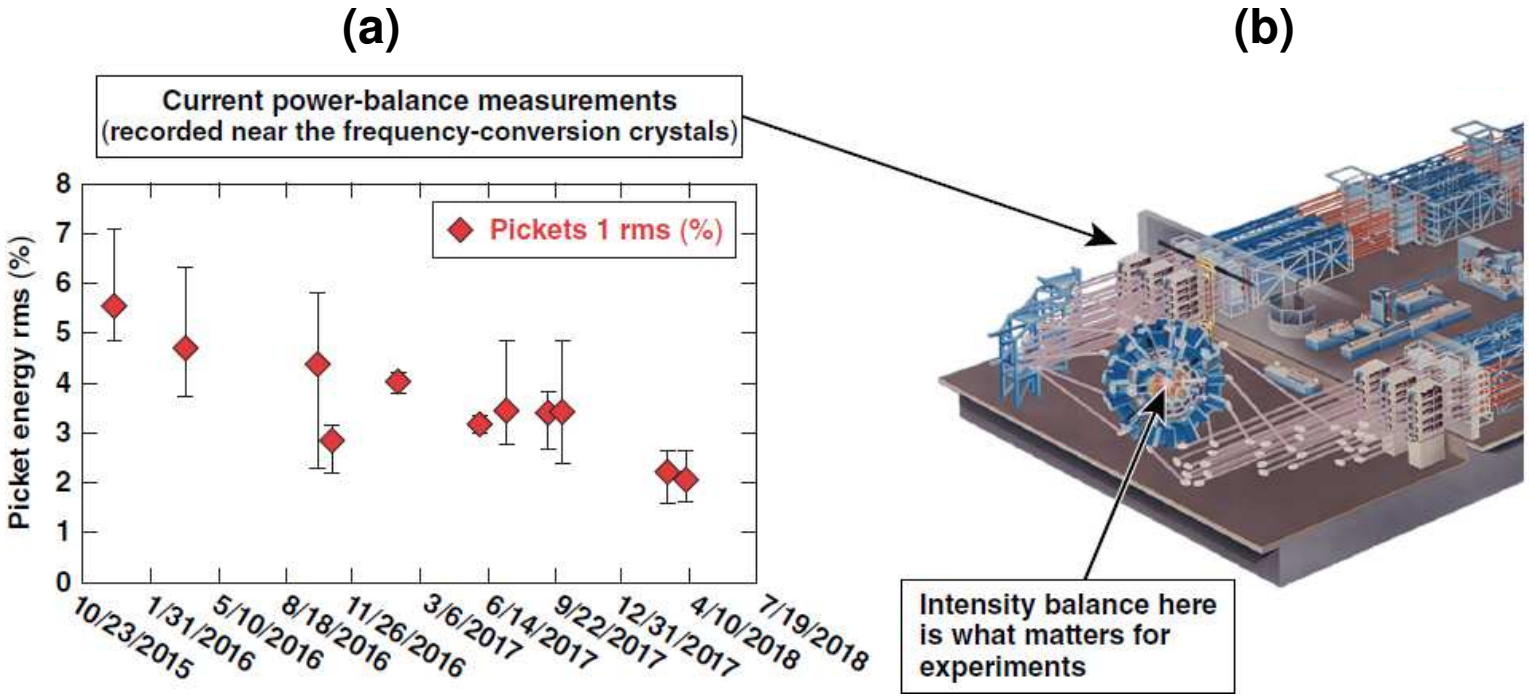
(a)
(b)
Current power-balance measurements
(recorded near the frequency-conversion crystals)
Pickets 1 rms (%)
Picket energy rms (%)
0
1
2
3
4
5
6
7
8
10/23/2015
1/31/2016
5/10/2016
8/18/2016
11/26/2016
3/6/2017
6/14/2017
9/22/2017
12/31/2017
4/10/2018
7/19/2018
Intensity balance here
is what matters for
experiments

Fig. 9

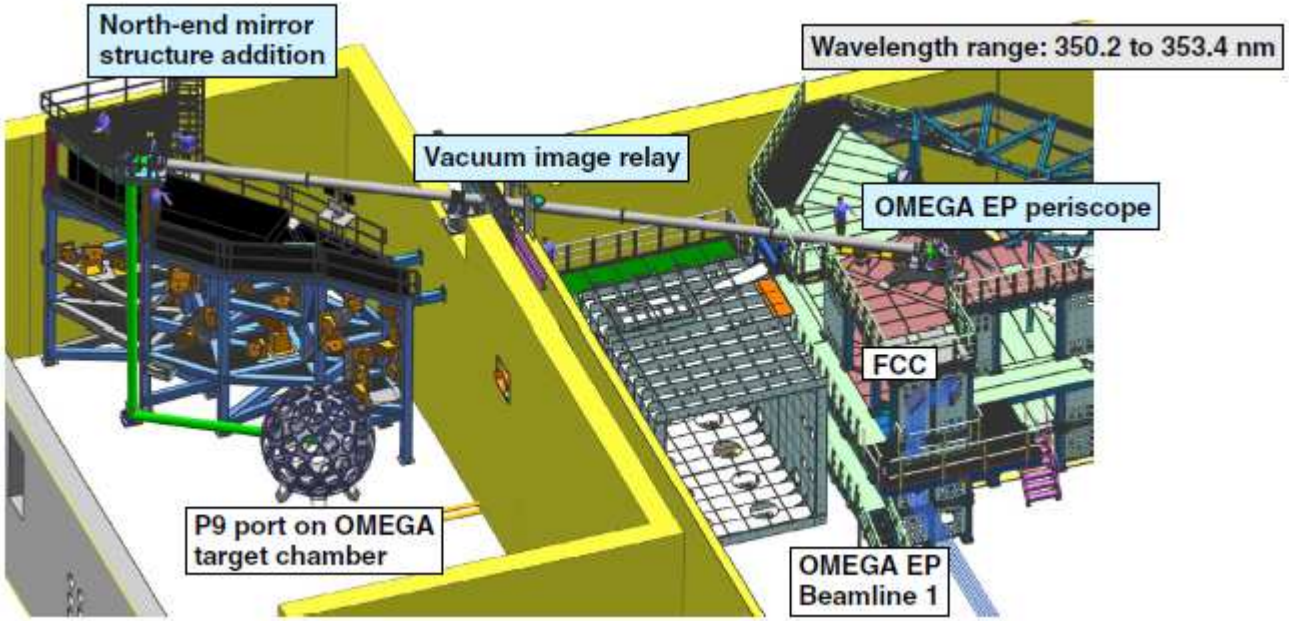
North-end mirror structure addition
Wavelength range: 350.2 to 353.4 nm
Vacuum image relay
OMEGA EP periscope
FCC
P9 port on OMEGA target chamber
OMEGA EP Beamline 1